Applied Energy 222 (2018) 649–661

Contents lists available at ScienceDirect

Applied Energy

journal homepage: www.elsevier.com/locate/apenergy

Economic justification of concentrating solar power in high renewable energy penetrated power systems

Ershun Du[a], Ning Zhang[a], Bri-Mathias Hodge[b], Chongqing Kang[a,*], Benjamin Kroposki[b], Qing Xia[a]

[a] State Key Lab. of Power System, Dept. of Electrical Engineering, Tsinghua University, Beijing 100084, China
[b] National Renewable Energy Laboratory, Golden, CO 80401, USA

HIGHLIGHTS

- We propose a novel method to perform the economic justification of CSP.
- CSP benefits include providing both renewable energy and operational flexibility.
- The break-even investment cost of CSP plants is analysed.
- Economic justifications of CSP in two provincial power systems in China are studied.
- CSP is much more competitive in power systems under high renewable penetrations.

ARTICLE INFO

Keywords:
Concentrating solar power
Variable renewable energy
Operational flexibility
Break-even cost
Economic justification

ABSTRACT

Concentrating solar power (CSP) plants are able to provide both renewable energy and operational flexibility at the same time due to its thermal energy storage (TES). It is ideal generation to power systems lacking in flexibility to accommodate variable renewable energy (VRE) generation such as wind power and photovoltaics. However, its investment cost currently is too high to justify its benefit in terms of providing renewable energy only. In this paper we evaluate the economic benefit of CSP in high renewable energy penetrated power systems from two aspects: generating renewable energy and providing operational flexibility to help accommodating VRE. In order to keep the same renewable energy penetration level during evaluation, we compare the economic costs between the system with a high share of VRE and another in which some part of the VRE generation is replaced by CSP generation. The generation cost of a power system is analyzed through chronological operation simulation over a whole year. The benefit of CSP is quantified into two parts: (1) energy benefit—the saving investment of substituted VRE generation and (2) flexibility benefit—the reduction in operating cost due to substituting VRE with CSP. The break-even investment cost of CSP is further discussed. The methodology is tested on a modified IEEE RTS-79 system. The economic justifications of CSP are demonstrated in two practical provincial power systems with high penetration of renewable energy in northwestern China, Qinghai and Gansu, where the former province has massive inflexible thermal power plants but later one has high share of flexible hydro power. The results suggest that the CSP is more beneficial in Gansu system than in Qinghai. The levelized benefit of CSP, including both energy benefit and flexibility benefit, is about 0.177–0.191 $/kWh in Qinghai and about 0.238–0.300 $/kWh in Gansu, when replacing 5–20% VRE generation with CSP generation.

1. Introduction

Increasing share of renewable energy sources (RES) in the generation mix of power systems creates additional variability and uncertainty that must be properly accommodated for economic and reliable system operations. Currently, wind power and photovoltaic (PV) generation capacities are rising quickly. By the end of 2016, the global installed capacity reached 487 GW for wind and 302 GW for PV [1]. In places of Demark, Ireland, Texas of U.S. and northwestern provinces in China, the penetration of RES has already reached a quite high level (serving more than 20% of total electricity demand) [2]. Wind power and PV generations are named variable renewable energy (VRE) because of the variability and uncertainty in their power outputs that are driven by prevailing weather conditions. The increasing integration of VRE may

* Corresponding author.
E-mail address: cqkang@tsinghua.edu.cn (C. Kang).

https://doi.org/10.1016/j.apenergy.2018.03.161
Received 14 December 2017; Received in revised form 29 March 2018; Accepted 30 March 2018

Nomenclature

Indices and sets

t	time index
i	thermal unit index
Ω_T	set of time periods for one day from t1 to t24
Ω_{Thm}	set of thermal units
Γ	set of time periods for the whole dispatching simulation time scope
f	subscript for thermal units that can start and stop daily
c	subscript for thermal units that cannot start and stop daily
h	subscript for hydro power units
w	subscript for VRE units
s	subscript for concentrating solar power plants

Parameters and constants

[1]	column vector which has unity elements
C_x	column vector of variable operational cost of unit type x, $x \in \{f,c,h,w,s\}$
C_d	column vector of load shedding cost
C_{wd}	column vector of VRE curtailment cost
V_f	column vector of start-stop costs of thermal units belonging to type f
C_{ave}	column vector of estimated average generating cost of power system
ΔP_{down}, ΔP_{up}	column vector of maximum and minimum ramp rates of generating units
$P_{\max}$, $P_{\min}$	column vector of maximum and minimum outputs of generating units
$P_w^{t,fore}$	column vector of forecasted VRE generation at time slot t
$P_s^{t,fore}$	column vector of available solar thermal power at time slot t
, $\eta^{PB}\eta^{TES}$	coefficients of power block efficiency and TES efficiency in CSP plants
D^t	column vector of nodal loads at time slot t
r_d^t, r_u^t	system up and down reserve requirements at time slot t
A_{ngx}	units and nodes incidence matrix of unit type x, $x \in \{f,c,h,w,s\}$
W	generation shifted distribution factor matrix
$F_{\max}$	column vector of transmission line capacity
$C_i(*)$	generation cost function of thermal unit i
$C_i^{fuel}(*)$	fuel cost function of thermal unit i
$C_i^{ramp}(*)$	ramp cost function of thermal unit i
$C_i^{su}(*)$	start-stop cost function of thermal unit i
a_i,b_i,c_i,d_t	coefficients of the cost function of thermal unit i
α	renewable energy generation penetration level
β	generation share of CSP in renewables
FCR	annual fixed charged ratio

Variable

S_f^t	column vector of start-stop cost of generating units belonging to type f
P_x^t	column vector of dispatched output of unit type x, $x \in \{f,c,h,w,s\}$
P_{wd}^t	column vector of VRE curtailed at time slot t
I_f^t	column vector of on/off status of thermal units with type f at time slot t
I_c	column vector of on/off status of thermal units belonging to type c
I_s^t	column vector of on/off status of CSP plants at time slot t
E_s^t	column vector of state of charge of TES in CSP plants at time slot t
$P_s^{cha,t}$	column vector of charging output of TES in CSP plants at time slot t
$P_s^{dis,t}$	column vector of discharging output of TES in CSP plants at time slot t
D_d^t	column vector of nodal load shedding at time slot t
P_i^t	output of thermal unit i at time slot t in the scenario without substituting VRE with CSP generation
$P_i^{t'}$	output of thermal unit i at time slot t in the scenario with substituting VRE with CSP generation
G_{VRE}	investment capacity of VRE in the scenario without substituting VRE with CSP
G'_{VRE}	investment capacity of VRE in the scenario with substituting VRE with CSP
G'_{CSP}	investment capacity of CSP in the scenario with substituting VRE with CSP
CSR_{CSP}	capacity substitute rate of CSP plants
LEB_{CSP}	levelized energy benefit of CSP generation
LFB_{CSP}	levelized flexibility benefit of CSP generation
LOB_{CSP}	levelized overall benefit of CSP generation
EB_{CSP}	overall energy benefits of CSP investment
FB_{CSP}	overall flexibility benefits of CSP investment
ROI_{CSP}	return of Investment for CSP plants
BEC_{CSP}	break-even cost of CSP plants

lead to additional requirements for operational reserves and ramping capacities, and thus reduce the operational benefit of renewable energy [3].

Power system operational flexibility denotes the ability of controllable generation units in changing their outputs to meet the variances of electricity loads, uncontrollable generation outputs and grid conditions. Since VRE generation is generally not dispatchable, net load is often used to evaluate the system operational flexibility requirement through treating VRE generation as negative load. Generally, the operational flexibility is provided by conventional fossil-fueled controllable generations, and the integration of VRE increases the requirement of operational flexibility.

Compared with wind and PV, concentrating solar power (CSP) plants are able to generate dispatchable renewable energy electricity [4,5]. Specifically, a CSP plant controls mirrors with tracking system to capture the direct normal irradiation (DNI) of sunlight which is then converted into thermal energy for utilization in a steam turbine to produce electricity. CSP plants allow for the incorporation of cost-efficient thermal energy storage (TES) to store the absorbed solar thermal energy for later use. This makes it possible for CSP to provide renewable energy and operational flexibility at the same time. The introduction of TES brings multiple benefits to CSP plants from several perspectives. First, since CSP plants can shift electricity generation using TES, it is capable of providing dispatchable generation and operational flexibility in power systems. Second, TES can remarkably increase the capacity factor of CSP through equipping larger solar collection fields, since surplus solar thermal energy can be stored in TES. Furthermore, TES systems in CSP plants are currently less costly (with capital costs around 20–70 $/kWh) than battery energy storage systems (with capital cost above $150/kWh) [6]. Compared with conventional thermal plants, CSP is generally regarded to be a semi-dispatchable technique due to the limit of absorbed solar energy [7].

Although the CSP development encounters some obstacles, such as much high capital cost and considerable land/water requirement, the advantages of CSP and the increasing need of renewable energy still attract widespread interests in CSP development [8]. E.g. CSP has considerable water requirements only when using wet-cooling, dry-cooling technique which significantly reduces the water demand is

becoming mature and is going to be used in new CSP projects [9]. Around the world, there is approximately 4800 MW of cumulative installed CSP capacity by the end of 2016 and nearly 20 GW of CSP projects in the pipeline [10]. Although CSP development is nascent, China is working on promoting CSP development and has announced a development target of 5 GW by 2020. Correspondingly, the Chinese government launched a feed-in tariff of 1.15 ¥/kWh for CSP generation and signed a series of demonstrative CSP projects with a total capacity of 1349 MW to support CSP development in 2016 [11].

Many previous studies have discussed the cost-benefit of CSP plants. Sioshansi and Denholm [12] analyse the revenue of a CSP plant with TES in a number of regions in the south-western United States and discussed the value of CSP net of capital costs. Madaeni et al. [13] further estimate the economic value of CSP in an electricity market considering the capacity value. Stoddard et al. [14] comprehensively analyse the economic, energy, and environmental benefits of CSP in California. In order to maximize the benefit of CSP, many mathematical models are proposed to optimize the operation strategy of CSP in electricity energy pool markets [15–17], while considering the uncertainties of solar irradiation and electricity prices. Kost et al. [18] compare the benefits of CSP plants under different price and support mechanisms. Generally, in majority of them, the CSP plant is assumed to be a price taker and operates with the target of maximizing its revenue in the electricity market. From the power system point of view, the CSP benefits of providing flexibility to accommodate more VRE and reducing the operational cost of conventional thermal generators have not been accounted.

Several studies have analysed the benefits of CSP in enhancing the system operational flexibility and promoting the integration of renewable energy. Santos et al. [19] study how to combine a wind farm with a CSP plant to provide stable renewable power generation. Chen et al. [20] reformulate the power system scheduling model to take CSP into consideration and analysed the benefit of CSP in reducing operating costs and VRE curtailment. Xu and Zhang [21] utilize a stochastic unit commitment model to simulate the operation of a power system with CSP and evaluated the value of CSP from the provision of providing energy and reserve services to integrate renewable energy. Denholm et al. [22] compare the economic value among CSP, base-load units, and PV based on a production simulation of the California power system with over 33% RE penetration, and further analysed the potential of enabling greater solar penetration via the use of CSP with TES [23]. Dominguez et al. [24] analyse the feasibility of operating a fully renewable electric energy system with CSP. Generally, these literatures evaluate the value of CSP through comparing the economics of a power system with and without CSP integration. However, the two cases involve different renewable penetration levels. This leads to an unfair comparison, since the system with higher renewable penetration generally has lower operational costs due to the nearly zero variable cost of renewable energy generation but higher overall costs due to the high investment cost of renewable energy power plants.

In this paper, we propose to analyse the economic justification of CSP in a power system with a high share of VRE generation through comparing its cost performance with another power system where part of the VRE generation is substituted with CSP generation while keeping the same penetration level of renewable energy. The benefits of CSP are divided into two parts: the provision of renewable energy, which is represented as the saved investments on substituted VRE generation, and the provision of operational flexibility, which is denoted as the reduction in operating costs when substituting VRE with CSP. In this study, the system operational flexibility is captured as the system operation cost to balance the net load (load minus renewable energy generation). A power system chronological operational simulation platform is used as the assessment tool in this paper. Finally, the value of TES and the break-even cost of CSP plants are analysed.

The rest of the paper is organized as follows. A qualitative discussion of the benefits of substituting part of the VRE generation with CSP generation are provided in Section 2. A simulation platform utilized for the analysis is introduced in Section 3. Section 4 presents an assessment framework to quantify the benefits of CSP for the provision of energy and operational flexibility. Numerical tests carried out on the modified IEEE-RTS system are presented in Section 5. The economic justifications of CSP investment in two provincial power systems in north-western China are studied in Section 6. Section 7 outlines the conclusions.

2. Benefit analysis of CSP integration

2.1. Overview

The fundamental difference between VRE and CSP is that CSP plants are dispatchable to serve loads in the same way as conventional thermal units when equipped with a thermal storage system. For power systems with a certain target of renewable energy generation penetration level, substituting part of the VRE generation with CSP generation could reduce the requirements on operational flexibility. The impacts of CSP integration on VRE plants, on thermal units and on power system economics are summarized in Fig. 1. The impacts of CSP are analysed from two perspectives: generating renewable energy and providing operational flexibility.

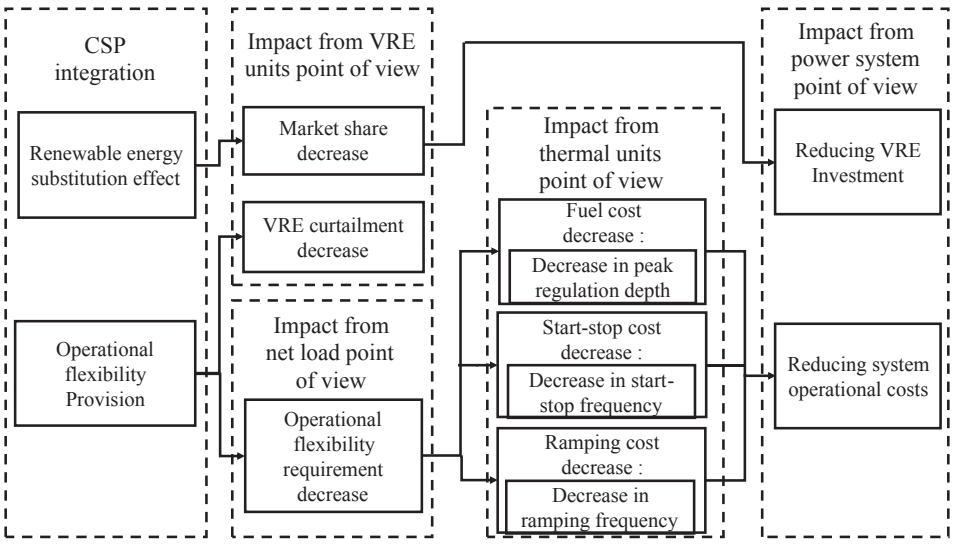

Fig. 1. Schematic diagram of the benefits of CSP integration for the provision of renewable energy and operational flexibility.

2.2. Energy benefit

The economic cost for a power system to achieve a pre-defined renewable energy penetration level can be divided into two parts: the investments in renewable energy power plants and the corresponding operational costs. Investing in CSP plants can substitute for investments in VRE, while maintaining the same level of renewable energy. Generally, per unit capacity of CSP will substitute for more than per unit capacity of VRE. This is because (1) the CSP plant has a higher capacity factor, since TES allows for CSP to incorporate a larger solar field and (2) the flexibility of CSP can partly compensate for the uncertainty and variability of VRE generation and thus decrease the amount of curtailed VRE generation. Therefore, even though the capital cost of CSP plants is higher than VRE plants, investing in CSP also may be better than only investing in VRE for achieving the pre-defined renewable energy penetration level. In this paper, the energy benefit of CSP integration is captured as the substituted investments in VRE.

2.3. Operational flexibility benefit

High penetrations of VRE largely increase the system operational flexibility requirement from many aspects, such as increasing the daily peak-valley difference of net load, and increasing the hourly variability and uncertainty of net load. On the contrary, the integration of CSP can reduce the system operational flexibility requirement from two aspects: (1) the CSP generation will substitute part of VRE generation, which brings down the operational flexibility needed to compensate the VRE generation uncertainty and variability and (2) the CSP generation can also provide additional operational flexibility so as to reduce the requirement of operational flexibility from conventional controllable generations.

Since smaller system operational flexibility requirement is generally involved with lower system operational costs, the operational flexibility benefit of CSP due to reducing the system operational flexibility requirement can be evaluated by the reduction in the system operational costs. Specifically, the reduction in system flexibility requirements will lead to changes in the behaviors of controllable generators (like thermal units) from many aspects such as peak-regulation depth, start-up frequency, and ramping frequency. These behavioral variations bring cost variations for thermal units in fuel costs, start-stop costs, and ramping costs, and lead to a cost reduction in the total system operational costs. This approach has been applied in the literature to analyze the economic cost of the additional system flexibility requirement for VRE integration [25].

3. Assessment tool: power system chronological operation simulation platform

3.1. Overall framework

The assessment tool used in this paper is a software designed for simulating the operation of a power system over a long time period. It is a sub-function of the software platform *Grid Optimization Planning Tool (GOPT),* which is a power system planning decision-making tool developed by Tsinghua University in China [26]. This software simulates the long term power system operation chronologically on a daily basis in order to evaluate the feasibility, reliability, and economics of the generation and transmission expansion scheme. The core of this simulation platform is a daily dispatching and scheduling module with security constrained unit commitment and economic dispatch (UCED) model. The simulation platform also contains a renewable energy production simulation module to generate wind power and PV outputs with hourly resolution based on the renewable energy planning scheme. The framework of the simulation platform is shown in Fig. 2, and the major modules in the platform are introduced in what follows.

3.2. Renewable energy production simulation module

This module produces chronological simulated time series data on the generation of wind plants, PV plants, and the solar thermal power production in the solar field of a CSP plant. These are used as an input to the daily operation simulation module. According to statistical data on historical wind speed and solar irradiation information, the module generates the chorological hourly sequences of wind speed and solar radiation through applying the methodology of stochastic differential equation proposed in [27], and further generates the chronological output of available electricity generation for wind and PV plants. For CSP plants, it utilizes the System Advisor Model (SAM) [28] to produce the chronological output of available solar thermal power based on the generated solar irradiation data.

3.3. Daily operation simulation module

This module simulates the daily operational dispatch of the generating units in a way that minimizes the operating cost while respecting the various constraints. All generation units are divided into five categories: thermal units that can be started and stopped daily (gas turbines and small thermal units), thermal units that cannot or should not be started or stopped daily (nuclear plants, large thermal unit and

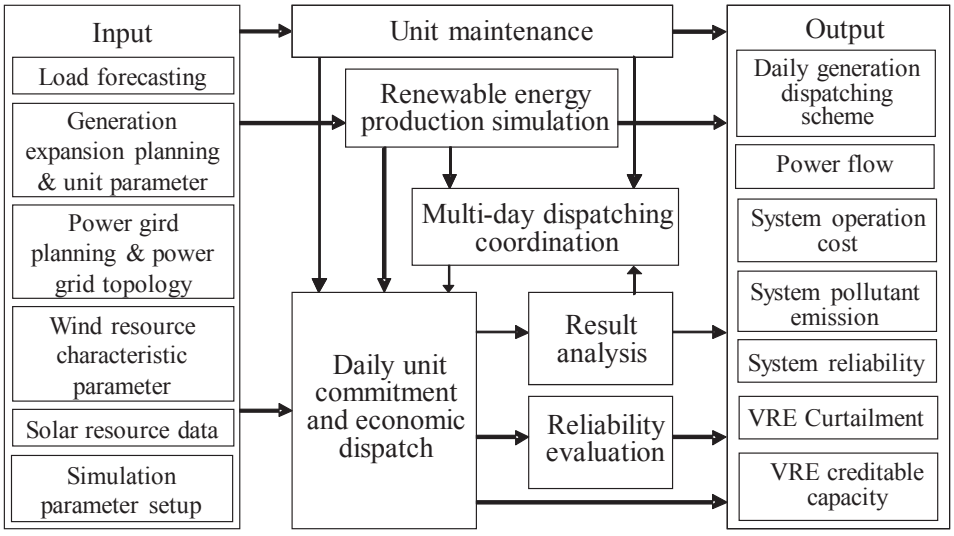

Fig. 2. Framework of power system chronological production simulation platform.

combined heat and power units), hydro plants, VRE plants, and CSP plants. These units are dispatched on an hourly basis according to a security constrained UC model.

$$\min C_{sys} = \sum_{t\in\Omega_T} (C_f^T P_f^t + C_c^T P_c^t + C_w^T P_w^t + C_h^T P_h^t + C_s^T P_s^t + C_{wd}^T P_{wd}^t + C_d^T D_d^t + [1]^T S_f^t) - C_{ave}^T E_s^{t_{|t=t24}}, \quad (1)$$

$$\text{s.t. } [1]^T P_f^t + [1]^T P_c^t + [1]^T P_h^t + [1]^T P_w^t + [1]^T P_s^t + [1]^T D_d^t = [1]^T D^t \quad \forall\ t\in\Omega_T, \quad (2)$$

$$[1]^T D^t + r_u^t [1]^T D^t \leqslant [1]^T P_{f,\max} * I_f^t + [1]^T P_{c,\max} * I_c + [1]^T P_{h,\max} + [1]^T P_{s,\max} * I_s^t + [1]^T P_w^t + [1]^T D_d^{t,fore} \quad \forall\ t\in\Omega_T, \quad (3)$$

$$[1]^T P_{f,\min} * I_f^t + [1]^T P_{c,\min} * I_c + [1]^T P_{s,\min} * I_s^t + [1]^T D_d^t \leqslant [1]^T D^t - r_d^t [1]^T D^t \quad \forall\ t\in\Omega_T, \quad (4)$$

$$P_{f,\min} * I_{f,\min}^t \leqslant P_{f,\max}^t \leqslant P_{f,\max} * I_f^t \quad \forall\ t\in\Omega_T. \quad (5)$$

$$P_{c,\min} * I_c \leqslant P_c^t \leqslant P_{c,\max} * I_c \quad \forall\ t\in\Omega_T. \quad (6)$$

$$-\Delta P_{f,down} \leqslant P_f^t - P_f^{t-1} \leqslant \Delta P_{f,up} \quad \forall\ t\in\Omega_T. \quad (7)$$

$$-\Delta P_{c,down} \leqslant P_c^t - P_c^{t-1} \leqslant \Delta P_{c,up} \quad \forall\ t\in\Omega_T. \quad (8)$$

$$(I_f^{t-1} - I_f^t) T_{f,off} + \sum_{j=t-T_{f,off}}^{t-1} (1 - I_f^j) \geqslant 0;$$
$$(I_f^t - I_f^{t-1}) T_{f,on} + \sum_{j=t-T_{f,on}}^{t-1} I_f^j \geqslant 0, \quad \forall\ t\in\Omega_T. \quad (9)$$

$$S_f^t \geqslant V_f * (I_f^t - I_f^{t-1}), \quad S_f^t \geqslant \mathbf{0} \quad \forall\ t\in\Omega_T. \quad (10)$$

$$P_w^t + P_{wd}^t = P_w^{t,fore}, \quad 0 \leqslant P_w^t, \quad 0 \leqslant P_{wd}^t, \quad \forall\ t\in\Omega_T. \quad (11)$$

$$P_{s,\min} * I_s^t \leqslant P_s^t \leqslant P_{s,\max} * I_s^t \quad \forall\ t\in\Omega_T. \quad (12)$$

$$-\Delta P_{s,down} \leqslant P_s^t - P_s^{t-1} \leqslant \Delta P_{s,up} \quad \forall\ t\in\Omega_T. \quad (13)$$

$$(I_s^{t-1} - I_s^t) T_{s,off} + \sum_{j=t-T_{s,off}}^{t-1} (1 - I_s^j) \geqslant 0;$$
$$(I_s^t - I_s^{t-1}) T_{s,on} + \sum_{j=t-T_{s,on}}^{t-1} I_s^j \geqslant 0, \quad \forall\ t\in\Omega_T, \quad (14)$$

$$P_s^t/\eta_s^{PB} + P_s^{cha,t} - P_s^{dis,t} \leqslant P_s^{t,fore} \quad \forall\ t\in\Omega_T. \quad (15)$$

$$E_s^t = E_s^{t-1} + \eta_s^{TES} P_s^{cha,t} - P_s^{dis,t}/\eta_s^{TES} \quad \forall\ t\in\Omega_T. \quad (16)$$

$$E_{s,\min} \leqslant E_s^t \leqslant E_{s,\max} \quad \forall\ t\in\Omega_T \quad (17)$$

$$P_{h,\min} \leqslant P_h^t \leqslant P_{h,\max} \quad \forall\ t\in\Omega_T \quad (18)$$

$$\sum_{t\in\Omega_T} P_h^t \leqslant Q_h^{hydro}. \quad (19)$$

$$-F_{\max} \leqslant WA_{ngf} P_f^t + WA_{ngc} P_c^t + WA_{ngh} P_h^t + WA_{ngw} P_w^t + WA_{ngs} P_s^t + WD_d^t - WD^t \leqslant F_{\max} \quad \forall\ t\in\Omega_T. \quad (20)$$

$$I_f^t \in \{0,1\}, \quad I_c \in \{0,1\}, \quad I_s \in \{0,1\} \quad \forall\ t\in\Omega_T. \quad (21)$$

$$D^t \geqslant D_d^t \geqslant \mathbf{0} \quad \forall\ t\in\Omega_T. \quad (22)$$

In the optimization model, the objective function (1) is the minimization of total system operating costs, including the energy costs, start-stop costs, and penalties for VRE curtailment and load shedding. P_f^t, P_c^t, P_h^t, P_w^t, P_{wd}^t, P_s^t, E_s^t, D_d^t, S_f^t, I_f^t and I_c are decision variables of the model. Since CSP can shift generation between different days through storing thermal energy in TES, the residual thermal energy of TES at the end of current operating day, denoted by $E_s^{t_{|t=t24}}$, is one of decision variables. The last item in objective function (1) denotes the estimated value of residual thermal energy in TES of CSP plants, where C_{ave} is the given system average generating cost. Constraints are set as follows. Eq. (2) is the load-generation balance constraint. Eqs. (3) and (4) are the system positive and negative reserve constraints. Eqs. (5) and (6) are generation output constraints; Eqs. (7) and (8) are thermal generation ramping rate constraints. Eq. (9) formulates the minimum on/off time period constraints for thermal units which are able to be started and stopped daily. Eq. (10) calculates the start-up cost of thermal units. Eq. (11) limits the generation of VRE plants. Eqs. (12)–(17) represent the operation of CSP plants with TES. Specifically, Eq. (12) and (13) are,

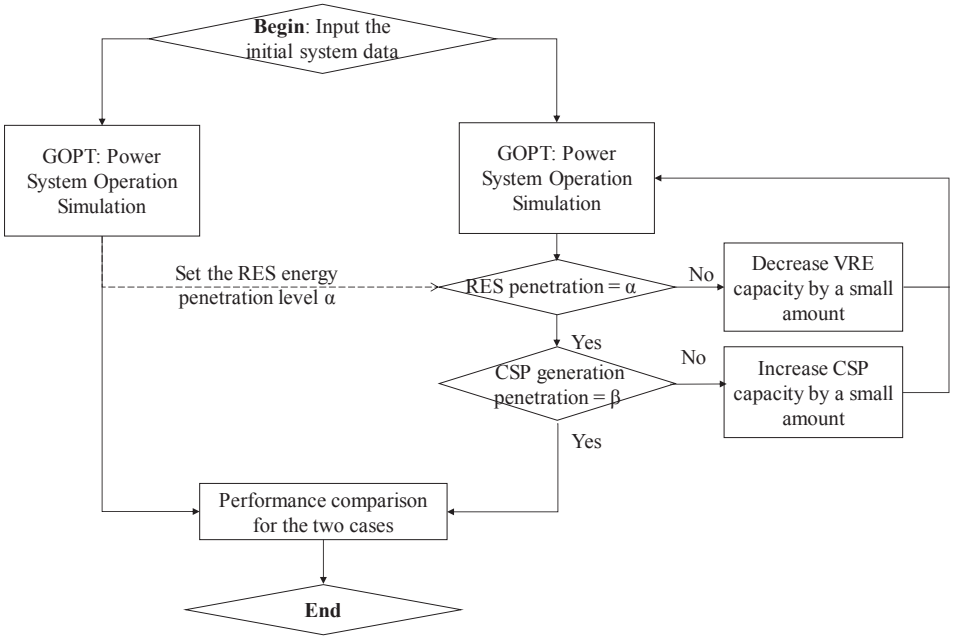

Fig. 3. Flow chart of assessing the benefit of CSP integration.

respectively, the generation output and the ramping rate constraints. Eq. (14) formulates the minimum on/off time period constraints. Eq. (15) represents the instantaneous thermal power balance, and Eq. (16) represents the power balance of the TES system. Eq. (17) limits the state of charge of TES systems. Eqs. (18) and (19) formulate the operation constraints of hydro units. Eq. (11) limits the generation of hydro units. Eq. (19) ensures that the overall generation of a hydro unit during one day is limited by the daily available generation Q_h^{hydro}. Before daily simulation, hydro units are dispatched first for peak shaving to decide the available generation Q_h^{hydro} for each day, subject to water flow during a month. Eq. (20) is the transmission capacity constraint for each branch. Eq. (22) limits the amount of load shedding.

This daily operation simulation model is a mixed integer linear programming (MILP) problem which is solved by the solver CPLEX [29]. The daily operation simulation is performed day by day to achieve a long-term operation simulation for power systems within a short solution time. A linear generation cost function for thermal units is adopted in the daily operation model. From the perspective of long-term power system operation simulation, the linear cost model for thermal plants are widely employed to shorten the simulation computation time [22,25]. The dispatching difference between a linear cost model and a quadratic curve model is deemed acceptable. It should be noted that the linear cost model is used only for dispatching purpose. A detailed cost model will be used to calculate the cost performance of thermal units in simulation post-processing. For CSP plants, a simplified MILP operation model formulated by Eqs. (11)–(15) is widely incorporated into the power system unit commitment model in many literatures [15–21], rather than a detailed but non-linear model proposed in [30] where only the operation of CSP is considered. The wind and solar generating forecasts are assumed to be perfect, which is also widely accepted in many literatures focusing on long-term power system operation simulation [18,22].

4. Benefit assessment framework and indices

4.1. Assessment framework

The benefit of CSP is evaluated by comparing the cost performances of power systems with and without CSP integration, while keeping the same RES penetration level (including VRE and CSP, excepting hydro). The assessment flow chart is shown in Fig. 3. We first simulate the operation of the power system that only has VRE plants and calculate the RES penetration level denoted by α. We then reduce the capacity of VRE and increase the capacity of CSP until the generation share of CSP in overall renewable energy generation is equal to β, while maintaining the RES penetration level unchanged as α. The cost performance and the installed capacity of renewable energy of the two power systems are compared. Performance indices on both the energy benefit and the operational flexibility benefit are introduced in detail in the following sub-sections.

4.2. Indices for energy benefit

The energy benefit of CSP comes from generating renewable energy and accommodating more VRE that otherwise may have to be curtailed. As discussed in Section 2.2, the energy benefit of CSP investment EB_{CSP} is quantified as the substituted VRE investment.

$$EB_{CSP} = IC(G_{VRE}) - IC(G'_{VRE}). \tag{23}$$

where G_{VRE} denotes the VRE capacity in the case without CSP, and G'_{VRE} denotes the VRE capacity in the case with CSP integration. Function $IC(*)$ denotes the annual fixed cost that includes the annualized capital investment cost and annual fixed operating cost. Taking VRE units as an example, the function $IC(G_{VRE})$ is formulated as follows.

$$IC(G_{VRE}) = FCR*CC_{VRE}*G_{VRE} + FC_{VRE}*G_{VRE}. \tag{24}$$

$$FCR = \frac{r(1+r)^n}{(1+r)^n - 1}. \tag{25}$$

where CC_{VRE} ($/kW) denotes the capital cost of VRE units, FC_{VRE} ($/kW-yr) is the annual fixed operating cost of VRE units, FCR is the annual fixed charge rate, r is the discount rate and n is the depreciation period.

Since the per unit investment cost of VRE may change at different times for different locations, a novel index called capacity substitution rate CSR_{CSP} is introduced to measure the energy benefit of CSP and is defined as the ratio of the substituted VRE capacity to the CSP capacity when replacing the same amount of VRE generation with CSP generation.

$$CSR_{CSP} = \frac{G_{VRE} - G'_{VRE}}{G'_{CSP}}. \tag{26}$$

where G'_{CSP} denotes the installed CSP capacity in the case with CSP integration

Furthermore, the energy benefit of CSP can be distributed to per unit CSP generation, which is called the levelized energy benefit (LEB) of CSP generation.

$$LEB_{CSP} = \frac{EB_{CSP}}{\sum_{t\in\Gamma}[1]^T P_s^t}. \tag{27}$$

where LEB_{CSP} denotes the value of LEB and $\sum_{t\in\Gamma}[1]^T P_s^t$ calculates the sum of CSP generation during the simulation year.

4.3. Indices for operational flexibility benefits

As discussed in Section 2.3, the variation in thermal generation operating costs caused by CSP integration can be mainly divided into three parts: fuel costs, ramping costs, and start-stop costs. These costs can be easily calculated through the results of the dispatch simulation.

A detailed cost function, shown in (28), is used to evaluate the cost performance of thermal units, which is the sum of a classical quadratic curve cost function and the ramp cost related with the absolute ramp rate.

$$\begin{aligned} C_i(P_i^t) &= C_{fi}(P_i^t) + C_{ri}(P_i^t) + C_{si}(I_i^t) \\ &= (a_i(P_i^t)^2 + b_i P_i^t + c_i) + d_i|P_i^t - P_i^{t-1}| + V_f*|I_f^t - I_f^{t-1}|. \end{aligned} \tag{28}$$

Eqs. (29)–(31) calculate the fuel cost savings, ramping cost savings, and start-stop savings of thermal units, respectively.

$$E_i^{fuel} = \sum_{t\in\Gamma} C_i^{fuel}(P_i^{t'}) - \sum_{t\in\Gamma} C_i^{fuel}(P_i^t). \tag{29}$$

$$E_i^{ramp} = \sum_{t\in\Gamma} C_i^{ramp}(P_i^{t'}) - \sum_{t\in\Gamma} C_{ri}(P_i^t). \tag{30}$$

$$E_i^{su} = \sum_{t\in\Gamma} C_i^{su}(I_i^{t'}) - \sum_{t\in\Gamma} C_i^{su}(I_i^t). \tag{31}$$

where E_i^{fuel}, E_i^{ramp} and E_i^{su} are the variations on fuel cost, ramping cost and start-stop cost for thermal plant i, respectively. $P_i^{t'}$ and P_i^t denote the generation output of thermal unit i at time period t in scenario with and without substituting CSP integration, respectively.

The operational flexibility benefit of CSP comes from reducing the system operational flexibility requirement. As discussed in Section 2, the operational flexibility benefit of CSP FB_{CSP} can be captured as the reduction on the system operation cost that is the sum of cost variations on fuel cost, ramping cost and start-stop cost for all thermal units.

$$FB_{CSP} = \sum_{i\in\Omega_{Thm}} (E_i^{fuel} + E_i^{ramp} + E_i^{su}). \tag{32}$$

Then, the operational flexibility benefit of CSP is distributed to per unit CSP generation, which is called the levelized flexibility benefit (LFB) of CSP generation.

$$LFB_{CSP} = \frac{FB_{CSP}}{\sum_{t\in\Gamma}[1]^T P_s^t}. \quad (33)$$

where LFB_{CSP} denotes the value of LFB.

4.4. Break-even cost of CSP

The overall benefit of CSP integration is the sum of the energy benefit and flexibility benefit. The levelized overall benefit (LOB) of CSP generation is calculated by:

$$LOB_{CSP} = LEB_{CSP} + LFB_{CSP}. \quad (34)$$

The cost-efficiency of CSP investment is a trade-off between the overall benefit and the corresponding CSP cost including capital cost, fixed operating cost and variable operating cost. Two indices return on investment and break-even cost, formulated by Eqs. (35) and (36), are utilized to evaluate the economics of CSP investment.

$$ROI_{CSP} = \frac{EB_{CSP} + FB_{CSP} - \sum_{t\in\Gamma} C_s^T P_s^t}{IC(G'_{CSP})}. \quad (35)$$

$$BEC_{CSP} = \frac{1}{FCR} * \left(\frac{EB_{CSP} + FB_{CSP} - \sum_{t\in\Gamma} C_s^T P_s^t}{G'_{CSP}} - FC_{CSP} \right). \quad (36)$$

where FC_{CSP} is the annual fixed operating cost of CSP plants. It should be noted that ROI_{CSP} larger than 100% or BEC_{CSP} larger than the capital cost of per unit capacity of CSP means the CSP investment is cost-efficient.

5. Case study: a modified IEEE RTS-79 test system

A modified IEEE RTS-79 system [31] with large scale of VRE integration is tested in this section to illustrate the benefits of CSP integration discussed above.

5.1. Basic data and settings

The IEEE RTS-79 test system is a typical system where thermal units represent a major proportion of the generation mix and handle the peak load, regulation, and ramping, shown in Table 1 and Fig. 4. Wind and PV plants are added to five nodes in the system with 200 MW at each node for each plant. The parameters of wind speed distribution and solar irradiation distribution are extracted from the Qinghai provincial system. The whole system has a maximum power demand of 2850 MW and yearly energy demand of 15.34 TWh. The installed VRE capacity reaches 70.2% of maximum demand. In this section, CSP generation is set to replace the VRE generation by 5%, 10%, 15% and 20%, respectively, while keeping the total amount of electricity generation from wind and solar unchanged. With the increase in CSP, the capacity of wind and PV is reduced equally. The cases with CSP share in renewables, β, equal to 0%, 5%, 10%, 15% and 20% are regarded as case 0, case 1, case 2, case 3 and case 4, respectively. The performances in cases 1 to 4 will be compared against case 0 to quantify the benefits of CSP integration for the provision of renewable energy and operational flexibility.

For the production simulation result of wind and PV, the average number of potential utilized hours in the year is 2086 h for wind plants and 1590 h for PV plants. The capital investment costs of wind and PV are set as 2000 $/kW and 2400 $/kW, respectively [32]. The fixed operating costs of wind and PV are set as 60 $/kW-yr and 40 $/kW-yr. The cost function of thermal units is quadratic and fitted according to the fuel price and fuel cost of different level of output provided in [31]. The ramping cost of all the thermal units are set at $5 per MW/h according to [33]. Systematic up- and down- reserve ratios are set at 5% and 2% of the load demand, respectively. For the sake of simplicity, unit maintenance is not considered. This system involves 38 transmission lines, and the transmission capacity constraints are considered in the simulation.

The parameters related to CSP plants are extracted from the Solar Advisor Model (SAM) [28]. A CSP plant consists of three interrelated components that can be sized independently, namely solar field, TES, and power block. The solar field, which concentrates solar irradiation to generate thermal power, is sized by its ratio of its rated thermal energy output to the rated thermal energy needs of its power block, which is named solar multiple (SM). The TES is sized by the number of hours that TES can be discharged to operate the power block at its rated capacity. In this study, five CSP plants are simulated and connected to the same locations with VRE plants. Their capacities are increased equally during the simulation. All of them are assumed to be equipped with 10-h TES and with a 2.4-SM solar field, which are the typical parameters of newly built CSP in China. Detailed parameters of CSP are listed in Table 2.

5.2. Simulation results

Table 3 summaries the simulation results of operating costs and VRE curtailment in each case. In the operation simulation result of case 0, the accommodated wind and PV generation is 3.39 TWh, making the renewable energy penetration level, α, equal to 22.1%. With the same α, substituting part of VRE generation with CSP generation leads to lower renewable energy capacity needed, lower system operational costs and lower VRE curtailment. Fig. 5 compares the scheduling of the power system with and without CSP on a certain week. The result shows that the dispatchability of CSP plants helps in shifting generation and brings less VRE curtailment. Specifically, from the view of daily operations, the CSP generation is shifted to the periods of sunrise and sunset. From the view of weekly operations, the CSP generation is shifted from Monday to Tuesday that is involved with high load but low wind/solar, and from the weekends to the working day in the next week. Since a large load drop in weekends, many on-line thermal units in Friday have to be shut-down. Therefore, the CSP generation is shifted from Wednesday and Thursday to Friday to reduce the on-line thermal units in Friday. This helps in saving start-up/shut-down costs of thermal units.

5.3. Benefits of CSP for providing renewable energy

Table 4 summarizes the indices of energy benefit of CSP proposed in Section 4.2. As expected, substituting more VRE with CSP leads to a greater reduction in the VRE capacity requirement and more benefits of CSP for the provision of renewable energy. The value of capacity substitution rate of CSP, CSR_{CSP}, is more than 2, suggesting that 1 MW of

Table 1
Generation mix and load data of the modified IEEE RTS-79 system.

Generation type	Unit group	Number	Capacity (MW)	Proportion (%)
Fossil-oil	U12	5	12 * 5	17.59
	U100	3	100 * 3	
	U197	3	197 * 3	
Fossil-coal	U76	4	76 * 4	23.57
	U155	4	155 * 4	
	U350	1	350 * 1	
Combustion turbine	U20	4	20 * 4	1.48
Nuclear	U400	2	800	14.80
Hydro	U50	6	300	5.55
Wind (new)	U_W	5	200 * 5	18.50
PV (new)	U_PV	5	200 * 5	18.50
Total	–	42	5405	100
Max load (MW)	2850			
Total load (TWh)	15.34			

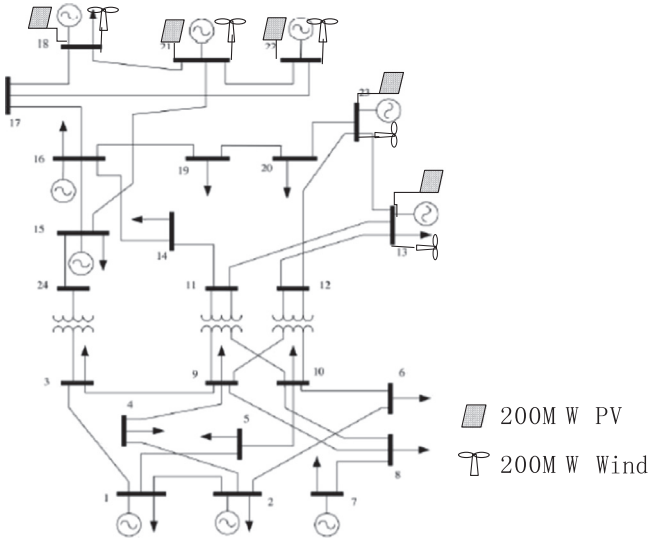

Fig. 4. Modified IEEE RTS-79 system.

CSP is able replace more than 2 MW of wind and PV in terms of energy production in this case. It is found that CSR_{CSP} decreases with the increase of β, the CSP share in renewables. This means that the marginal benefit of CSP decreases with higher CSP penetration.

5.4. Benefits of CSP for providing operational flexibility

In order to compare the system flexibility requirement in each case, we compare the characteristics of system net load under different CSP capacity. Fig. 6 shows the duration curve of hourly load ramps and Fig. 7 shows the duration curve of peak-valley difference in each day with different CSP capacities. Obviously, the CSP decreases the hourly load ramp and daily load peak-valley difference. Two statistic indices are used to quantify the variation, namely the mean value and 95% quantile value and are shown in Table 5. Taking case 4 (β = 20%) as an example, the average hourly load ramp drops from 53 MW to 45.9 MW with 13.4% reduction, and the average peak valley difference drops from 768 MW to 682 MW, an11.2% reduction.

We compare the variations in thermal generation operational costs in case 0 to case 4 to analyze the benefits of substituting VRE with CSP from the view of reducing the system flexibility requirement. Table 6 shows the thermal generation cost reductions in fuel costs, ramping costs, and start-stop costs, and calculates the percentage of each part. The result shows that CSP is able to bring down thermal generation costs. It should be noted that the energy produced by thermal generation maintains the same in different cases so that the cost reduction is from better operating point and less ramps. Numerically, fuel cost reductions are the dominated contributor (with over 75%), while ramping cost reductions occupies the smallest part (about 5%). Notably, with the increase of CSP share in RES generation, the share of fuel cost reduction increases and the other two parts go down.

Table 7 calculates the reduction percentage of thermal generation cost due to CSP integration. The result shows that the ramp cost and start-stop cost has a significant reduction with the integration of CSP.

In order to further understand the changes in the operation of thermal generation, Fig. 8 calculates the utilization hour variation for different types of thermal units for each scenario. From the results we can see that CSP integration leads to an increase in utilization hours for large thermal plants U350 and U400 which are cheap but relatively inflexible, and leads to decreases in utilization hours for small thermal plants like U197, U100 and U20 which are relatively flexible but expensive. The change of the utilization hours in different thermal generation is the main reason for the system fuel cost reductions.

The reduction of average thermal generation cost and the levelized

Table 3
Simulation results of IEEE RTS-79 system in each case.

		Case 0	Case 1	Case 2	Case 3	Case 4
Energy generation mix	Hydro	8.46%	8.48%	8.49%	8.51%	8.53%
	Thermal	69.44%	69.47%	69.40%	69.36%	69.35%
	RES	*22.09%*	*22.05%*	*22.11%*	*22.13%*	*22.12%*
	Wind in RES	54.3%	53.2%	50.4%	47.6%	44.9%
	PV in RES	45.7%	41.9%	39.6%	37.3%	35.0%
	CSP in RES	*0.0%*	*5.0%*	*10.0%*	*15.1%*	*20.1%*
Capacity (MW)	Wind	1000	930	870	812	757
	PV	1000	930	870	812	757
	CSP	0	58	118	177	234
	Total	2000	1918	1858	1801	1748
Annual operation cost (M$)	Total	800.5	796.9	793.3	789.7	784.6
	Fuel	791.0	788.3	784.6	782.6	778.1
	Ramp	3.20	2.98	2.81	2.64	2.53
	Start-up	6.26	5.61	5.03	4.46	3.92
VRE curtailment		7.81%	5.71%	4.17%	2.95%	2.04%

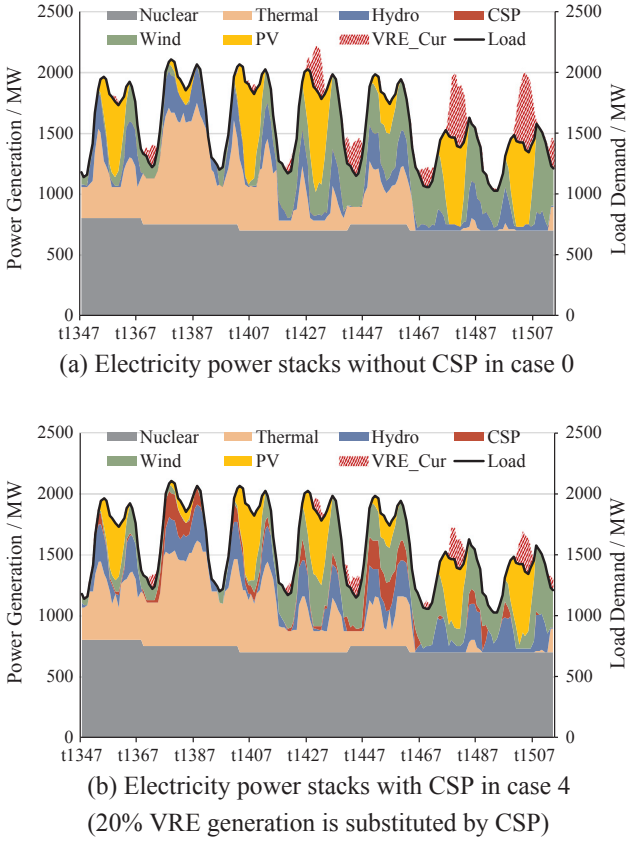

Fig. 5. Comparison of power balance with and without CSP on a certain week.

Table 2
Parameters of CSP plants.

Parameter	Solar multiple	TES capacity	Minimum output	Ramping limit	Minimum on/off time	η^{PB}	η^{TES}
Value	2.4	10 h	40%	40%	2 h	38%	98%

Table 4
Energy benefits of CSP in case 1 to case 4 compared with case 0.

CSP share in renewables	β = 5%	β = 10%	β = 15%	β = 20%
Substituted VRE capacity (MW)	140	260	376	486
Investment capacity of CSP (MW)	58	118	177	234
Energy benefits of CSP: EB_{CSP} (M$)	37.80	70.20	101.52	131.22
CSP capacity substitution rate: CSR_{CSP}	2.414	2.203	2.124	2.077
Levelized energy benefit: LEB_{CSP} ($/kWh)	0.225	0.206	0.198	0.193

flexibility benefit of CSP generation are compared and shown in Fig. 9. From the results, we can see that (1) the levelized flexibility benefit of CSP generation LFB_{CSP} keeps almost the same level by 0.021 $/kWh and is much higher than the reduction of average thermal generation cost and (2) the reduction of average thermal generation cost goes up with the increase of CSP penetration level β.

5.5. Break-even cost of CSP

Table 8 shows the cost-benefit analysis of substituting VRE with CSP. Fig. 10 shows the composition of the benefits. The cost settings of CSP are 5300 $/kW for capital cost, 50 $/kW-yr for fixed operating cost and 0 $/kWh for variable operating cost [32]. The value of *FCR* is assumed to be 0.10 (8% discount rate and 20 yeas depreciation period). From the result we can see that: (1) the cost of CSP investment can be paid back in all the cases, (2) the break-even cost of CSP decreases with the increase of β, the CSP share in renewables, (3) the benefits of the provision of renewable energy is the dominated benefit contributor with about 90%, and (4) the share of the benefits from reducing the system flexibility requirement increases with the increasing integration of CSP.

5.6. Sensitivity to the CSP investment cost

The cost performance of renewable energy is determinant to the cost efficiency of substituting VRE with CSP. Literature shows that the future costs of CSP technology are expected to decrease significantly [34]. We perform the cost-benefit analysis of CSP with two sets of renewable energy cost data in the USA for 2050 from a NREL report [32]. Here the incremental technology improvement (ITI) scenario and evolutionary technology improvement (ETI) are both considered in Table 9. Fig. 11 shows the results of a cost-benefit analysis of CSP in all three cases, including the previous renewable energy cost performance in 2020. With the cost reduction of VRE investment, the break-even cost of CSP involves a considerable drop in 2050. Since CSP cost will also experience a great drop in 2050, the return on investment of CSP remains nearly the same in the 2050 ITI scenario and involves a significant increase in the 2050 ETI scenario.

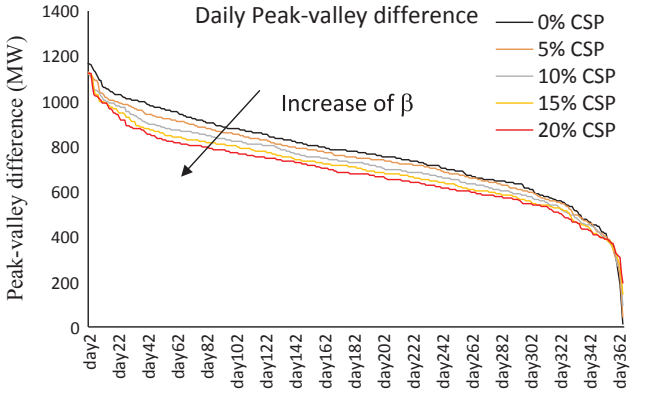

Fig. 7. Duration curves of the daily peak-valley difference of net load with different CSP shares in renewables.

Table 5
Statistics of net load in different cases.

	(MW)	Case 0	Case 1	Case 2	Case 3	Case 4
Hourly load ramp up	Mean	53.02	51.16	49.15	47.44	45.91
	q(95%)	270.38	261.26	250.69	244.53	236.69
Hourly load ramp down	Mean	53.07	51.21	49.19	47.49	45.95
	q(95%)	222.17	219.46	213.83	210.08	209.24
Peak valley difference	Mean	767.6	746.4	721.2	699.8	682.2
	q(95%)	1,040.9	1,006.1	994.4	973.3	958.2

Table 6
Thermal generation cost variation in IEEE RTS-79 case.

CSP share in renewables	β = 5%	β = 10%	β = 15%	β = 20%
Flexibility benefits of CSP: FB_{CSP} (M$)	3.55	7.23	10.75	15.89
Saving in fuel costs (M$)	2.68(75.5%)	5.60(77.6%)	8.39(78.0%)	12.89(81.1%)
Saving in ramp costs (M$)	0.217(6.1%)	0.388(5.4%)	0.555(5.2%)	1.81(4.2%)
Saving in start-up costs (M$)	0.65(18.4%)	1.23(17.1%)	1.81(16.8%)	2.35(14.8%)

5.7. Sensitivity to the TES capacity

The capacity of the TES system in the CSP plant is the chief determinant of the operational flexibility of CSP and thus has a significant impact on the cost-efficiency of CSP. Table 10 shows the results of a cost-benefit analysis of CSP with different TES capacities in case 2 (substituting 10% VRE

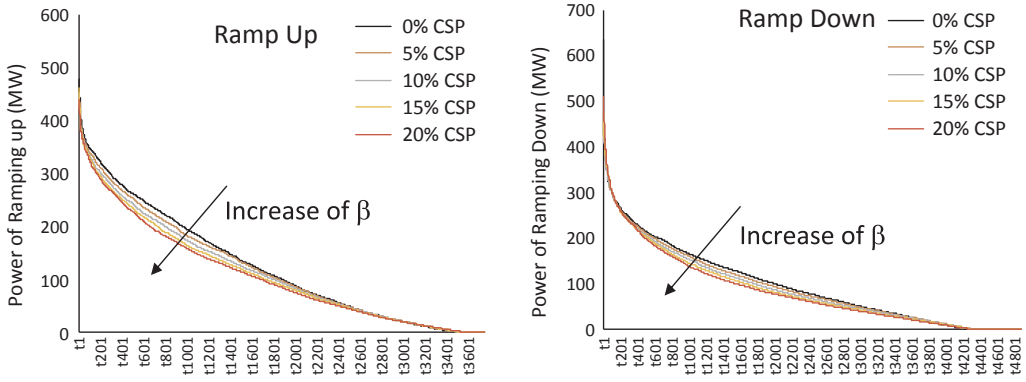

Fig. 6. Duration curves of the hourly net load ramp with different CSP shares in renewables.

Table 7
The percentage of thermal generation cost reductions.

CSP shares in renewables	β = 5%	β = 10%	β = 15%	β = 20%
Reduction in overall operational costs	0.58%	1.25%	1.70%	2.40%
Reduction in fuel costs	0.34%	0.81%	1.06%	1.63%
Reduction in ramp costs	6.08%	12.15%	17.36%	20.67%
Reduction in start-up costs	10.43%	19.69%	28.89%	37.49%

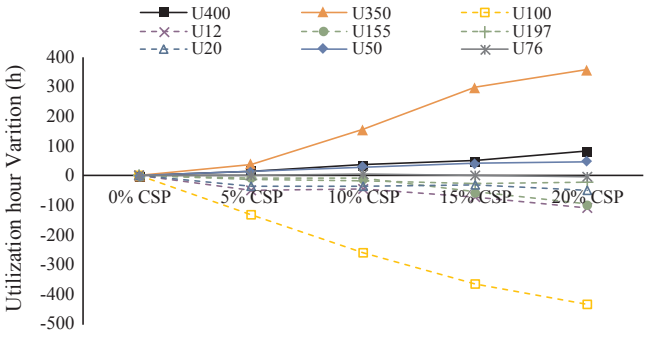

Fig. 8. Utilization hour variation for different units in IEEE RTS-79 system with different CSP shares in renewables.

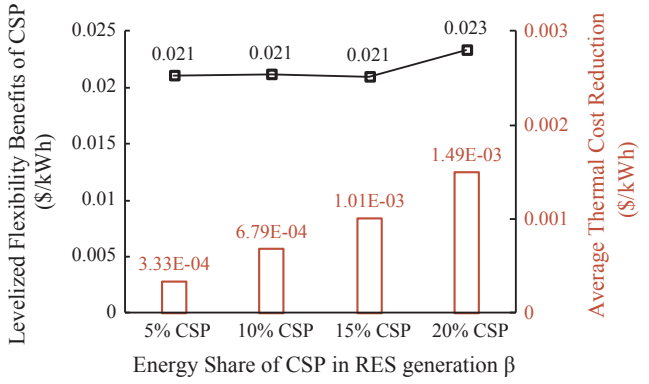

Fig. 9. Levelized flexibility benefit of CSP and average generation cost reduction of thermal units with different CSP shares in renewables.

Table 8
Cost-benefit analysis of CSP integration in IEEE RTS-79 case.

CSP share in renewables	β = 5%	β = 10%	β = 15%	β = 20%
Sum of energy and flexibility benefits (M$)	41.3	77.4	112.3	147.1
Levelized overall benefit of CSP LOB_{CSP} ($/kWh)	0.246	0.227	0.219	0.216
Annualized capital cost of CSP (M$)	30.74	62.54	93.81	124.02
Annual fixed operating cost of CSP (M$)	2.9	5.9	8.85	11.7
Return on investment: ROI_{CSP}	123%	113%	109%	108%
Break-even cost of CSP: BEC_{CSP} ($/kW)	6629	6062	5843	5787

generation with CSP). Obviously, with the decrease of TES capacity, the CSP capacity substitution rate CSR_{CSP} drops rapidly and the VRE curtailment ratio increases. As expected, the economic benefits of CSP, namely EB_{CSP} and FB_{CSP}, both decrease with the reduction of TES capacity, which leads to a sharp drop in the break-even cost of CSP. Specifically, when no TES is installed, the value of CSR_{CSP} nearly drops to one and the benefits in reducing system flexibility requirements drops to near zero, which makes the break-even cost of CSP drop to 2618 $/kW.

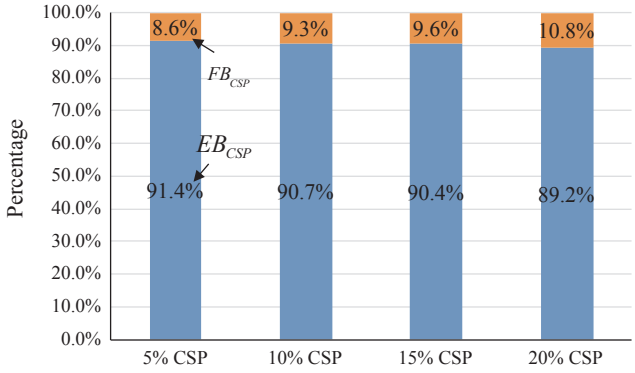

Fig. 10. The composition of the benefits of substituting VRE with CSP.

Table 9
Investment cost of renewable technologies.

		Wind	PV	CSP
Capital cost ($/kW)	2020 Scenario	2000	2400	5300
	2050 ITI	2000	2000	4700
	2050 ETI	1800	1700	2950
Fixed operating cost ($/kW-yr)	2020 Scenario	60	40	50
	2050 ITI	60	30	50
	2050 ETI	10	10	45

6. Empirical analysis in North-western China

The two provincial power systems of Qinghai and Gansu in the northwestern China are analysed in this section with the addition of CSP. The data for these two power systems comes from the generation and transmission expansion planning scheme and load forecasting data in 2020. These two provinces are both located in an area with high quality solar resources and are suitable for large scale CSP development. Qinghai system is dominated by hydro power and thus associated with relative adequate operational flexibility, while Gansu system is dominated by thermal units and faces severe VRE shedding problems.

6.1. Qinghai provincial power system in 2020

6.1.1. Basic data

The data used in this case comes from one of the electric power planning blueprint of Qinghai province of China in 2020, in which 3 GW of wind power and 10 GW of PV are planned to be installed. The capacity mix and load forecasting data in this plan is shown in Table 11, from which we can see that hydro plants make up the major proportion. It is forecasted that in 2020 the whole system will have a peak load of 15.8 GW and a total electric energy consumption of 113 TWh. The installed VRE capacity reaches 82.3% of maximum load demand.

Data related to wind and PV outputs are obtained from existing historical generation database. The data related to CSP generation is from SAM. The cost function of the thermal units is quadratic. The ramping cost of all the thermal units are set at $5 (33.33 ¥) per MWh. Constraints of transmission capacity is not considered. Other simulation settings are the same as the case IEEE RTS-79 test system.

6.1.2. Simulation results

The same procedure for IEEE RTS-79 system has been performed for the Qinghai provincial power system. The simulation results are summarized in Table 12. The share of electricity generation from solar and wind is kept constant at 18.7%. As expected, the case with higher CSP penetration level is involved with lower renewable energy capacity investment, lower system operational costs and lower VRE curtailment.

Table 13 shows the cost-benefit analysis of substituting VRE with

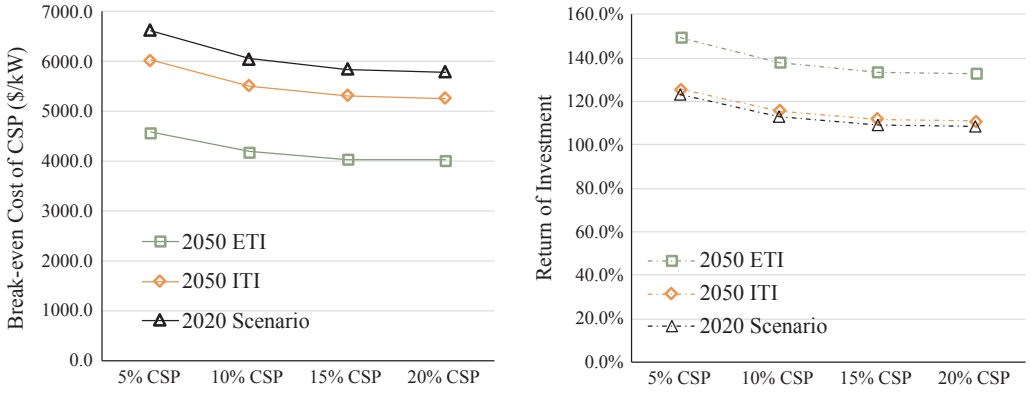

Fig. 11. Break-even cost and return of investment of CSP in IEEE RTS-79 case under three renewable energy cost scenarios.

Table 10
Cost-benefit analysis of CSP with different TES capacities.

TES capacity	0 h	5 h	10 h	15 h
Substituted VRE capacity (MW)	235	258	260	260
Investment capacity of CSP (MW)	204	128	118	113
CSP capacity substitution rate: CSR_{CSP}	1.152	2.016	2.203	2.301
VRE curtailment ratio	5.35%	4.22%	4.17%	4.12%
Energy benefits of CSP: EB_{CSP} (M$)	63.45	69.66	70.20	70.20
Flexibility benefits of CSP: FB_{CSP} (M$)	0.16	6.38	7.23	7.83
Return of investment: ROI_{CSP}	62.4%	110.0%	113.1%	111.4%
Break-even cost of CSP: BEC_{CSP} ($/kW)	2618	5441	6062	6405

Table 11
Generation mix and load forecasting data of Qinghai system in 2020.

Generation type	Number	Capacity (MW)	Proportion (%)
Fossil-coal	30	12,010	29.94%
Hydro	62	15,096	37.63%
Wind power	12	3000	7.48%
PV	64	10,008	24.95%
Total	166	40,114	100.00%
Max load (MW)	15,800		
Total load (TWh)	113		

Table 12
Simulation results of Qinghai system in each case.

		Case 0	Case 1	Case 2	Case 3	Case 4
Energy generation mix	Hydro	30.8%	30.8%	30.7%	30.7%	30.7%
	Thermal	50.5%	50.5%	50.6%	50.6%	50.6%
	RES	*18.7%*	*18.7%*	*18.7%*	*18.7%*	*18.7%*
	Wind in RES	29%	27%	26%	24%	23%
	PV in RES	71%	68%	64%	61%	57%
	CSP in RES	*0%*	*5%*	*10%*	*15%*	*20%*
Capacity (MW)	Wind	3000	2838	2682	2529	2379
	PV	10,008	9468	8947	8437	7936
	CSP	0	355	710	1065	1415
Operation cost (M$)	Total	11.941	11.871	11.848	11.828	11.799
	Fuel	11.813	11.744	11.725	11.712	11.687
	Ramp	0.0885	0.0878	0.0876	0.0843	0.0831
	Start-up	0.0396	0.0385	0.0359	0.0315	0.0293
VRE curtailment		0.68%	0.34%	0.15%	0.06%	0.02%

Table 13
Cost-benefit analysis of CSP in Qinghai system.

CSP share in renewables	5%	10%	15%	20%
Substituted VRE capacity (MW)	702	1379	2042	2693
Investment capacity of CSP (MW)	355	710	1065	1415
CSP capacity substitution rate: CSR_{CSP}	1.979	1.942	1.918	1.903
Energy benefits of CSP: EB_{CSP} (M$)	189.657	372.289	551.409	727.017
Flexibility benefits of CSP: FB_{CSP} (M$)	10.582	13.941	16.972	21.308
Levelized overall benefit of CSP: LOB_{CSP} ($/kWh)	0.191	0.183	0.179	0.177
Annualized capital cost (M$)	188.15	376.3	564.45	749.95
Annual fixed operating cost (M$)	17.75	35.5	53.25	70.75
Return on investment: ROI_{CSP}	97.3%	93.8%	92.0%	91.2%
Break-even cost of CSP: BEC_{CSP} ($/kW)	5141	4940	4837	4789

Table 14
Generation mix and load forecasting data of Gansu system in 2020.

Generation type	Number	Capacity (MW)	Proportion
Fossil-oil	56	51,047	58.09%
Fossil-coal	60	9853	11.21%
Combustion turbine	25	19,970	22.73%
Nuclear	7	7002	7.97%
Total	166	87,872	100.00%
Max load (MW)	25,860		
Total load (TWh)	158		

Table 15
Simulation results of Gansu system in each case.

		Case 0	Case 1	Case 2	Case 3	Case 4
Energy generation mix	Hydro	28.7%	28.8%	28.9%	28.9%	28.9%
	Thermal	43.4%	43.3%	43.3%	43.2%	43.1%
	RES	*27.9%*	*27.9%*	*27.9%*	*27.9%*	*27.9%*
	Wind in RES	77%	75%	71%	67%	64%
	PV in RES	23%	20%	19%	18%	16%
	CSP in RES	*0%*	*5%*	*10%*	*15%*	*20%*
Capacity (MW)	Wind	19,970	18,273	16,875	15,696	14,578
	PV	7002	6407	5917	5504	5111
	CSP	0	750	1480	2170	2870
Operation cost (M$)	Total	25.585	25.277	25.177	24.984	24.797
	Fuel	25.14	24.87	24.80	24.62	24.44
	Ramp	0.241	0.220	0.216	0.212	0.210
	Start-up	0.2022	0.1853	0.1639	0.1495	0.1445
VRE curtailment		10.89%	8.38%	7.81%	6.49%	5.01%

Table 16
Cost-benefit analysis of CSP in Gansu system.

CSP share in renewables	5%	10%	15%	20%
Substituted VRE capacity (MW)	2293	4181	5772	7282
Investment capacity of CSP (MW)	750	1480	2170	2870
CSP capacity substitution rate: CSR_{CSP}	3.057	2.825	2.660	2.537
Energy benefits of CSP: EB_{CSP} (M$)	619.00	1128.78	1558.44	1966.26
Flexibility benefits of CSP: FB_{CSP} (M$)	46.25	61.24	90.19	118.16
Levelized overall benefit of CSP: LOB_{CSP} ($/kWh)	0.300	0.269	0.252	0.238
Annualized capital cost of CSP (M$)	397.5	784.4	1150.1	1521.1
Annual fixed operating cost of CSP (M$)	37.5	74	108.5	143.5
Return on investment: ROI_{CSP}	152.9%	138.6%	131.0%	125.2%
Break-even cost of CSP: BEC_{CSP} ($/kW)	8370	7541	7097	6763

CSP. From the result, we can see that the capacity substitution ratio CSR_{CSP} decreases with the increase of CSP share in renewables and is relatively small at around 1.9. Since the system is dominated by hydro power, the flexibility benefits of CSP are much lower than the benefits for the provision of renewable energy. In general, the break-even cost of CSP decreases with the increase of β. With the cost setting (2000 $/kW for wind, 2400 $/kW for PV and 5300 $/kW for CSP), the value of ROI_{CSP} indicates that the CSP investment is not cost-efficient in all of the cases.

6.2. Gansu provincial power system in 2020

6.2.1. Basic data

The data used in this case comes from one of the electric power planning blueprint of Gansu province of China in 2020, in which 20 GW of wind power and 7 GW of PV are planned to be installed. The capacity mix and load forecasting data in this plan is shown in Table 14, from which we can see that thermal plants make up the major proportion. It is forecasted that in 2020 the whole system will have a peak load of 25.86 GW and a total electric energy consumption of 158 TWh. The installed VRE capacity reaches 104.3% of maximum load demand. Simulation settings are the same as the case on Qinghai system.

Table 15 shows the simulation results with different CSP shares in renewables. The share of electricity generation from solar and wind keeps constant at 27.9%. As expected, the case with higher CSP share (larger β) is involved with lower renewable energy capacity investment, lower system operational costs, and lower VRE curtailment. Table 16 shows the cost-benefit analysis of substituting VRE with CSP. From this result we can see that the capacity substitution ratio CSR_{CSP} decreases with the increase of β and is relatively large at between 2.5 and 3.0. With such a high renewable energy penetration level, the Gansu system is facing severe VRE curtailment problem. In this light, substituting VRE with CSP will be very cost-efficient. With the cost setting (2000 $/kW for wind, 2400 $/kW for PV and 5300 $/kW for CSP), the results of ROI_{CSP} show that the CSP investment can be paid back in all cases, and the break-even cost of CSP is much higher than that for Qinghai system.

7. Conclusions

This paper provides new insights into the benefits of CSP integration for the provision of renewable energy and operational flexibility. A power system operation simulation platform is used to analyze the economic justification of CSP plants in high renewable energy penetrated power systems. Compared with the current studies which focus on analyzing the benefits of CSP for selling energy and reserves in an electricity market or for the coordination with VRE to facilitate the integration of VRE, we propose a model to analyze the benefits of CSP from the perspective of power system operation through substituting part of the VRE generation with CSP production, while keeping the same renewable generation penetration level. Specifically, we are able to quantify the benefits of CSP from two aspects: (1) energy benefit which is calculated by the investment cost of substituted VRE capacity and (2) flexibility benefit which is reflected by the reduction of system operating costs.

Some conclusions can be drawn from the simulation results: (1) The CSP investment is more cost-efficient in a power system with deficient system operational flexibility and severe VRE curtailment problems, such as the Gansu system. (2) The marginal benefits of CSP decrease with the increasing proportion of substituting VRE with CSP. (3) Substituting VRE with CSP brings considerable reductions in thermal generation fuel costs, ramping costs, and start-stop costs, in which the fuel cost reductions are the dominated contributor. (4) The cost-efficiency of CSP is quite sensitive to the TES capacity. (5) The levelized overall benefit of CSP generation is about 0.177–0.191 $/kWh in Qinghai system and about 0.238–0.300 $/kWh in Gansu system, when replacing 5–20% VRE generation with CSP generation. These results could provide a reference for the planning-making on the CSP development and the reasonable configuration of CSP.

From the analysis results, CSP plants may play a significant role for power systems towards renewable-dominated and minimum-cost targets. In future work, the optimal renewable energy generation mix is explored to achieve high renewable penetrations.

References

[1] Renewable Energy Policy Network for the 21st Century (REN21). Global Status Report 2016 < http://www.ren21.net/wp-content/uploads/2016/06/GSR_2016_FullReport_.pdf > .
[2] Kroposki B, Johnson B, Zhang Y, et al. Achieving a 100% renewable grid: operating electric power systems with extremely high levels of variable renewable energy. IEEE Power Energy Magazine 2017;15(2):61–73.
[3] Ummels BC, Gibescu M, Pelgrum E, Kling WL, Brand AJ. Impacts of wind power on thermal generation unit commitment and dispatch. IEEE Trans Energy Conv 2007;22(1):44–51.
[4] International Energy Agency (IEA). Technology roadmap: concentrating solar power; 2010 < http://www.iea.org/publications/freepublications/publication/csp_roadmap.pdf > .
[5] Desideri U, Zepparelli F, Morettini V, et al. Comparative analysis of concentrating solar power and photovoltaic technologies: technical and environmental evaluations. Appl Energy 2013;102(2):765–84.
[6] Zhao H, Wu Q, Hu S, et al. Review of energy storage system for wind power integration support. Appl Energy 2015;137:545–53.
[7] Vasallo MJ, Bravo JM. A MPC approach for optimal generation scheduling in CSP plants. Appl Energy 2016;165:357–70.
[8] Janjai S, Laksanaboonsong J, Seesaard T. Potential application of concentrating solar power systems for the generation of electricity in Thailand. Appl Energy 2011;88(12):4960–7.
[9] Bracken N, Macknick J, Tovar-hastings A, et al. Concentrating solar power and water issues in the U.S. southwest. National Renewable Energy Laboratory, Tech. Rep. NREL/TP-6A50-61376, March 2015.
[10] Renewable Energy Policy Network for the 21st Century (REN21). Renewables global status report; 2017 < http://www.ren21.net/wp-content/uploads/2017/06/170607_GSR_2017_Full_Report.pdf > .
[11] Du E, Zhang N, Kang C, et al. Reviews and prospects of the operation and planning optimization for grid integrated concentrating solar power. Proc CSEE 2016;36(21):5765–75. [in Chinese].
[12] Sioshansi R, Denholm P. The value of concentrating solar power and thermal energy storage. IEEE Trans Sustain Energy 2010;1(3):173–83.
[13] Madaeni SH, Sioshansi R, Denholm P. Estimating the capacity value of concentrating solar power plants with thermal energy storage: a case study of the southwestern United States. IEEE Trans Power Syst 2013;28(2):1205–15.
[14] Stoddard L, Abiecunas J, Connell RO. Economic, energy, and environmental benefits of concentrating solar power in California. National Renewable Energy Laboratory, Tech. Rep. NREL/SR-550-39291, April 2006.
[15] Dominguez R, Baringo L, Conejo AJ. Optimal offering strategy for a concentrating solar power plant. Appl Energy 2012;98:316–25.
[16] Pousinho HMI, Contreras J, Pinson P, Mendes VMF. Robust optimization for self-scheduling and bidding strategies of hybrid CSP-fossil power plants. Int J Electr Power Energy Syst 2015;67:639–50.
[17] Petrollese M, Cocco D, Cau G, Cogliani E. Comparison of three different approaches for the optimization of the CSP plant scheduling. Solar Energy 2017;150:463–76.
[18] Kost C, Flath CM, Möst D. Concentrating solar power plant investment and operation decisions under different price and support mechanisms. Energy Policy 2013;61:238–48.
[19] Santos-Alamillo FJ, Pozo-Vazquez D, Ruiz-Arias JA, et al. Combining wind farms with concentrating solar plants to provide stable renewable power. Renew Energy 2015;76:539–50.
[20] Chen R, Sun H, Li Z, Liu Y. Grid dispatch model and interconnection benefit analysis

of concentrating solar power plants with thermal storage. Autom Electr Power Syst 2014;38(19):1–7. [in Chinese].
[21] Xu T, Zhang N. Coordinative commitment and dispatch of concentrated solar power and wind resources to provide energy and reserve Services. IEEE Trans Power Syst 2017;32(2):1260–71.
[22] Denholm P, Wan Y, Hummon M, Mehos M. Analysis of concentrating solar power with thermal energy storage in a California 33% Renewable Scenario. NREL/TP-6A20-58186. Golden (CO): National Renewable Energy Laboratory; 2013.
[23] Denholm P, Mehos M. Enabling greater penetration of solar power via the use of CSP with thermal energy storage. NREL/TP-6A20-52978. Golden (CO): National Renewable Energy Laboratory; 2013.
[24] Dominguez R, Conejo AJ, Carrion M. Operation of a fully renewable electricity energy system with CSP plants. Appl Energy 2014;119:417–30.
[25] Zhang N, Kang C, Kirschen DS, et al. Thermal generation operating cost variations with wind power integration, in: Power and energy society general meeting. IEEE; 2011. p. 1–8.
[26] Power system planning decision-making and evaluation system GOPT technical manual. Beijing: Department of Electrical Engineering, Tsinghua University; 2010.
[27] Zhang N, Kang C, Duan C, et al. Simulation methodology of multiple wind farms operation considering wind speed correlation. Int J Power Energy Syst 2010;30(4):264–73.
[28] System Advisor Model (SAM). National renewable energy laboratory. [EB/OL] < https://sam.nrel.gov/ > .
[29] IBM ILOG. CPLEX Optimizer; 2010.
[30] Usaola J. Operation of concentrating solar power plants with storage in spot electricity markets. IET Renew Power Gener 2012;6(1):59–66.
[31] Grigg C, et al. IEEE reliability test system. IEEE Trans Power Apparat Syst 1979;2(98):2047–54.
[32] Hand M, Baldwin S, De EM, et al. Renewable electricity futures study, vol. 4. NREL/TP-6A20-52409. Golden (CO): National Renewable Energy Laboratory; 2012.
[33] Hamal C, Sharma A. Adopting a ramp charge to improve performance of the Ontario market [Online] < http://www.ieso.ca/imoweb/pubs/consult/mep/MP_WG-20060707-ramp-cost.pdf > .
[34] Hernández-Moro J, Martínez-Duart JM. Analytical model for solar PV and CSP electricity costs: present LCOE values and their future evolution. Renew Sustain Energy Rev 2013;20(4):119–32.